

GSA Data Repository and Supplemental Information for

Subtropical coral reveals abrupt early 20th century freshening in the western North Pacific Ocean

Thomas Felis*, Atsushi Suzuki, Henning Kuhnert, Mihai Dima, Gerrit Lohmann, Hodaka Kawahata

*To whom correspondence should be addressed. E-mail: tfelis@uni-bremen.de

Supporting Material and Methods

Coral records. Core OGA-02-1 was drilled vertically from the top of a massive *Porites* colony at Miyanohama on the north coast of Chichijima in the Ogasawara Islands (Japan) on 27 October 2002, using a diver-operated pneumatic drill. The core is without gap over its total length of 1.74 m. Individual segments fit seamlessly.

Microsampling, $\delta^{18}\text{O}$ and $\delta^{13}\text{C}$ analyses, age model construction and bimonthly interpolation followed methods described previously (Felis et al., 2004). More than 7 samples/year on average were obtained. For chronology construction annual $\delta^{18}\text{O}$ maxima were set to February/March; on average the coolest months. The maximum difference between annual $\delta^{18}\text{O}$ maxima and those in Sr/Ca and U/Ca is one data point. A shorter core (OGA-02-3) was drilled horizontally from the colony's side, and analysed for stable isotopes following methods described previously (Suzuki et al., 2005).

For Sr/Ca and U/Ca analyses a 250-300 μg split of the sample powder that was used for stable isotope analyses was digested in 2% HNO_3 and measured on a ThermoFinnigan Element2 High-Resolution Inductively Coupled Plasma Mass Spectrometer at Bremen University. Elemental concentrations were determined on ^{43}Ca , ^{87}Sr and ^{238}U ; with ^{89}Y as internal standard. Repeated measurements of a laboratory coral standard allowed offline correction for instrumental drift. Internal precisions were better than 0.2% relative standard error (RSE) for Ca and Sr, and 0.3% RSE for U. After a year, 45 samples were measured in duplicate from new splits; the average differences between two replicates were 0.04 mmol/mol for Sr/Ca and 0.02 $\mu\text{mol/mol}$ for U/Ca.

We did not use the coral record's 1995-2002 interval for climate reconstruction due to a breakdown of the Sr/Ca and U/Ca paleothermometers. Although $\delta^{18}\text{O}$, Sr/Ca, U/Ca and $\delta^{13}\text{C}$ over this youngest growth interval show clear annual cycles, annual average Sr/Ca and U/Ca values indicate apparently low temperatures, in conflict with high Chichijima sea surface temperature (SST) during this period (Figs. DR6, DR7). A Sr/Ca paleothermometer breakdown during recent decades has also been observed in other studies (Liu et al., 2005; Marshall and McCulloch, 2002). We think that the breakdown is due to thermal stress (Marshall and McCulloch, 2002) resulting from extraordinarily high SST in the second half of the 1990s to early 2000s, which is consistent with coral bleaching and mortality at Chichijima in 1998 (The Japanese Coral Reef Society and Ministry of the Environment, 2004). However, gridded SST estimates identify these recent temperature extremes as unique over the coral's lifetime, implying that the coral paleothermometers before this interval are free of thermal-stress-related problems. This is supported by impressive correlations between annual average local

SST and coral Sr/Ca ($r = -0.66$) and U/Ca ($r = -0.61$) respectively during the calibration period (99.5% level, 2-sided t-test).

Calibrations and reconstructions. For proxy calibration, the annual Sr/Ca maxima and minima were tied to the corresponding extreme values in a local monthly SST record from Chichijima (1975-1994, Tokyo Metropolitan Ogasawara Fisheries Center). A linear least-squares regression was then carried out for bimonthly interpolated Sr/Ca and SST data (SST defined as independent variable), giving a relationship of:

$$\text{Sr/Ca} \times 10^3 = 10.333(\pm 0.078) - 0.051(\pm 0.003) \times \text{SST} \quad (r^2 = 0.66)$$

The same procedure was applied to the U/Ca and $\delta^{18}\text{O}$ records, giving relationships of:

$$\text{U/Ca} \times 10^6 = 2.057(\pm 0.500) - 0.034(\pm 0.002) \times \text{SST} \quad (r^2 = 0.68)$$

$$\delta^{18}\text{O} = -0.642(\pm 0.140) - 0.158(\pm 0.006) \times \text{SST} \quad (r^2 = 0.85)$$

Relationships for annual average data are:

$$\text{Sr/Ca} \times 10^3 = 12.453(\pm 0.880) - 0.140(\pm 0.037) \times \text{SST} \quad (r^2 = 0.44)$$

$$\text{U/Ca} \times 10^6 = 3.259(\pm 0.608) - 0.084(\pm 0.026) \times \text{SST} \quad (r^2 = 0.37)$$

$$\delta^{18}\text{O} = 0.689(\pm 1.547) - 0.213(\pm 0.065) \times \text{SST} \quad (r^2 = 0.37)$$

The slopes of the equations derived from regression of coral proxies (Sr/Ca, U/Ca, $\delta^{18}\text{O}$) on local SST (measured in nearby Futami Bay) are similar to those of *Porites* calibrations at other locations (Corrège et al., 2000; Felis et al., 2004; Gagan et al., 1998; Marshall and McCulloch, 2002; Min et al., 1995; Suzuki et al., 2005). Compared to bimonthly data, the regression slopes are different for annual average data.

Differences in the slope relation between seasonal and annual regressions have been widely reported for coral $\delta^{18}\text{O}$ (Crowley et al., 1999). However, our annual regression slope for $\delta^{18}\text{O}$ is within the range documented for *Porites* (Evans et al., 2000). The annual regression slopes for Sr/Ca and U/Ca imply an apparent amplification of inferred

SST variations on interannual and longer timescales, which has also been observed in coral Sr/Ca records at other locations (Linsley et al., 2006). Differences in the slope relation between seasonal and annual regressions are most likely due to coral physiology and calcification.

The $\Delta\delta^{18}\text{O}$ was calculated following conventional methods (Gagan et al., 1998) using annual average data and annual regression equations. This approach is more convenient for reconstructing $\Delta\delta^{18}\text{O}$ changes on interannual and longer timescales compared to using seasonal data and seasonal regression equations. We note that the slope of our annual coral $\delta^{18}\text{O}$ -SST regression is not significantly affected by variations in $\delta^{18}\text{O}$ of seawater, as indicated by its value within the typical range for *Porites* (Evans et al., 2000) and the lack of correlation between annual average local SST and regional SSS (Carton and Giese, 2008) ($r = 0.03$). Similarly, a multiple linear regression between annual average coral $\delta^{18}\text{O}$, local SST and regional SSS ($\delta^{18}\text{O} = -0.214 \times \text{SST} + 0.387 \times \text{SSS} - 12.756$) indicates that the SSS effect on interannual coral $\delta^{18}\text{O}$ variability is negligible (0.2%) compared to the SST effect (37.4%) during the calibration period.

As an alternative procedure for estimating the magnitude of the 1905-1910 freshening in terms of psu, we carried out linear least-squares regressions for annual coral $\Delta\delta^{18}\text{O}$ and regional SSS (Carton and Giese, 2008) (1958-1994, SSS defined as independent variable), giving relationships of $\Delta\delta^{18}\text{O}_{\text{Sr/Ca}} = -75.967(\pm 18.503) + 2.184(\pm 0.532) \times \text{SSS}$ ($r^2 = 0.32$) and $\Delta\delta^{18}\text{O}_{\text{U/Ca}} = -97.802(\pm 27.954) + 2.812(\pm 0.803) \times \text{SSS}$ ($r^2 = 0.26$). This procedure results in a much smaller magnitude (0.14 ± 0.02 psu decrease in SSS) compared to that derived from applying the $\delta^{18}\text{O}_{\text{seawater}}$ -salinity relationship of the region (Schmidt et al., 1999) (0.82 ± 0.01 psu decrease in SSS). At the moment, we consider the latter procedure as more robust, as the correctness of the

amplitude of the reanalysis SSS data remains to be shown. We note that a newer version of the reanalysis SSS data (SODA 2.0.2-3) prior to 1965 diverges from the version used here. However, the reason for this divergence in the two reanalysis products is beyond the scope of this paper. More importantly, independent of including or excluding the period prior to 1965, the similarity between our two coral $\Delta\delta^{18}\text{O}$ records and reanalysis SSS is impressive on interannual to decadal timescales (Fig. 2). Complementary $\Delta\delta^{18}\text{O}$ records based on combining annual coral $\delta^{18}\text{O}$ with gridded SST estimates reveal similar results with respect to timing and magnitude of the freshening (Fig. DR7). This holds also true when alternative methods for reconstructing $\Delta\delta^{18}\text{O}$ from coral $\delta^{18}\text{O}$ and Sr/Ca (U/Ca) are applied (Cahyarini et al., 2008; Ren et al., 2002) (not shown).

Error bars for annual average coral records (Fig. 2A-B) were calculated using the corresponding analytical error of a single measurement (± 0.04 mmol/mol for Sr/Ca, ± 0.02 $\mu\text{mol/mol}$ for U/Ca, $\pm 0.07\text{‰}$ for $\delta^{18}\text{O}$), which reduces to ± 0.016 mmol/mol (Sr/Ca), ± 0.008 $\mu\text{mol/mol}$ (U/Ca) and $\pm 0.029\text{‰}$ ($\delta^{18}\text{O}$) because an annual average value is calculated from 6 independent measurements (Bevington and Robinson, 2003). Error bars for annual coral $\Delta\delta^{18}\text{O}$ records (Fig. 2C) were calculated following the procedures described by (Cahyarini et al., 2008) using the slopes of the annual coral proxy-SST regression equations and analytical errors reported above. The resulting error is $\pm 0.038\text{‰}$ for coral $\Delta\delta^{18}\text{O}_{\text{Sr/Ca}}$ and $\pm 0.035\text{‰}$ for coral $\Delta\delta^{18}\text{O}_{\text{U/Ca}}$, or, ± 0.09 psu and ± 0.08 psu, respectively, when the regional $\delta^{18}\text{O}_{\text{seawater}}$ -salinity relationship is applied ($0.42\text{‰}/1$ psu) (Schmidt et al., 1999).

For 3 yr running averages of the annual records of coral Sr/Ca, U/Ca and $\Delta\delta^{18}\text{O}$ shown in Fig. 2, correlations are significant (2-sided t-test) at 95% between SST and

coral Sr/Ca ($r = -0.87$) and coral U/Ca ($r = -0.84$) respectively; and at 99.5% between SSS and coral $\Delta\delta^{18}\text{O}_{\text{Sr/Ca}}$ ($r = 0.83$) and coral $\Delta\delta^{18}\text{O}_{\text{U/Ca}}$ ($r = 0.76$) respectively.

SLP difference maps. For generating the SLP difference maps, anomalies were calculated from the Global Mean Sea Level Pressure data set GMSLP2 (Basnett and Parker, 1997) (1871-1994). Winter, summer and annual SLP fields were calculated and linear trends were removed. The periods 1873-1905 and 1910-1942 were separated and individually detrended, to avoid projection from interdecadal/multidecadal variability on the mean. The difference map of average SLP fields for 1910-1942 minus average SLP fields for 1873-1905 was calculated, revealing the SLP pattern associated with the 1905-1910 freshening.

Supporting Text

Significance of freshening shift. Changes in coral physiology or calcification rate are not responsible for the 1905-1910 shift towards more negative coral $\delta^{18}\text{O}$, because no simultaneous shift is observed in coral $\delta^{13}\text{C}$ (a proxy for metabolic activity) or growth rate (a proxy for calcification) (Fig. DR7). A shift towards higher growth rate following the coral $\delta^{18}\text{O}$ shift by about 5 years could represent a response to the reconstructed freshening, but cannot have induced the $\delta^{18}\text{O}$ shift via so-called kinetic isotope effects. Furthermore, the average coral growth rate of 1.2 cm/year is well beyond the critical value of 0.6 cm/year, where kinetic isotope effects on *Porites* $\delta^{18}\text{O}$ become dominant (Felis et al., 2003). Finally, changes in coral physiology or calcification rate would have simultaneously affected all coral proxies, which is not observed.

Diagenetic alteration of the coral skeleton is not responsible for the 1905-1910 shift towards more negative coral $\delta^{18}\text{O}$, because thin-section and scanning-electron-

microscope analyses reveal excellent preservation of primary porosity in the lowermost core section. No secondary aragonite cements are observed in the skeletal pore spaces (Figs. DR8, DR9). Finally, diagenetic alteration of the 1873-1905 core section would have simultaneously affected all coral proxies in the same sense, which is not observed.

Slight deviations from the coral's major growth axis in the lowermost core section are within the range of other studies (Felis et al., 2000; Linsley et al., 2004; Ren et al., 2002) and are not responsible for the 1905-1910 shift towards more negative coral $\delta^{18}\text{O}$. The worst case scenario of analysing $\delta^{18}\text{O}$ along a section of horizontal coral growth (1983-1994) revealed average values (-4.44‰) nearly identical to those from a contemporaneous section of vertical growth (-4.38‰) (Fig. DR10), with both sections having similar growth rates (1.3 and 1.4 cm/year). This indicates that effects of growth axis changes on coral $\delta^{18}\text{O}$ are negligible in this colony.

References cited

- Basnett, T.A., and Parker, D.E., 1997, Development of the Global Mean Sea Level Pressure Data Set GMSLP2, Hadley Centre Climate Research Technical Note CRTN 79.
- Bevington, P.R., and Robinson, K.D., 2003, Data reduction and error analysis for the physical sciences, McGraw-Hill Higher Education, 336 p.
- Cahyarini, S.Y., Pfeiffer, M., Timm, O., Dullo, W.-C., and Garbe-Schönberg, D., 2008, Reconstructing seawater $\delta^{18}\text{O}$ from paired coral $\delta^{18}\text{O}$ and Sr/Ca ratios: Methods, error analysis and problems, with examples from Tahiti (French Polynesia) and Timor (Indonesia): *Geochimica et Cosmochimica Acta*, v. 72, p. 2841-2853.

- Carton, J.A., and Giese, B.S., 2008, A Reanalysis of Ocean Climate Using Simple Ocean Data Assimilation (SODA): *Monthly Weather Review*, v. 136, p. 2999-3017.
- Corrège, T., Delcroix, T., Récy, J., Beck, W., Cabioch, G., and Le Cornec, F., 2000, Evidence for stronger El Niño-Southern Oscillation (ENSO) events in a mid-Holocene massive coral: *Paleoceanography*, v. 15, p. 465-470.
- Crowley, T.J., Quinn, T.M., and Hyde, W.T., 1999, Validation of coral temperature calibrations: *Paleoceanography*, v. 14, p. 605-615.
- Evans, M.N., Kaplan, A., and Cane, M.A., 2000, Intercomparison of coral oxygen isotope data and historical sea surface temperature (SST): Potential for coral-based SST field reconstructions: *Paleoceanography*, v. 15, p. 551-563.
- Felis, T., Lohmann, G., Kuhnert, H., Lorenz, S.J., Scholz, D., Pätzold, J., Al-Rousan, S.A., and Al-Moghrabi, S.M., 2004, Increased seasonality in Middle East temperatures during the last interglacial period: *Nature*, v. 429, p. 164-168.
- Felis, T., Pätzold, J., and Loya, Y., 2003, Mean oxygen-isotope signatures in *Porites* spp. corals: inter-colony variability and correction for extension-rate effects: *Coral Reefs*, v. 22, p. 328-336.
- Felis, T., Pätzold, J., Loya, Y., Fine, M., Nawar, A.H., and Wefer, G., 2000, A coral oxygen isotope record from the northern Red Sea documenting NAO, ENSO, and North Pacific teleconnections on Middle East climate variability since the year 1750: *Paleoceanography*, v. 15, p. 679-694.
- Gagan, M.K., Ayliffe, L.K., Hopley, D., Cali, J.A., Mortimer, G.E., Chappell, J., McCulloch, M.T., and Head, M.J., 1998, Temperature and surface-ocean water

balance of the mid-Holocene tropical western Pacific: *Science*, v. 279, p. 1014-1018.

Gedalof, Z., Mantua, N.J., and Peterson, D.L., 2002, A multi-century perspective of variability in the Pacific Decadal Oscillation: new insights from tree rings and corals: *Geophysical Research Letters*, v. 29, 2204, doi: 10.1029/2002GL015824.

Ghil, M., Allen, M.R., Dettinger, M.D., Ide, K., Kondrashov, D., Mann, M.E., Robertson, A.W., Saunders, A., Tian, Y., Varadi, F., and Yiou, P., 2002, Advanced spectral methods for climatic time series: *Reviews of Geophysics*, v. 40, doi: 10.1029/2001RG000092.

Linsley, B.K., Kaplan, A., Gouriou, Y., Salinger, J., deMenocal, P.B., Wellington, G.M., and Howe, S.S., 2006, Tracking the extent of the South Pacific Convergence Zone since the early 1600s: *Geochemistry, Geophysics, Geosystems*, v. 7, Q05003, doi: 10.1029/2005GC001115.

Linsley, B.K., Wellington, G.M., Schrag, D.P., Ren, L., Salinger, M.J., and Tudhope, A.W., 2004, Geochemical evidence from corals for changes in the amplitude and spatial pattern of South Pacific interdecadal climate variability over the last 300 years: *Climate Dynamics*, v. 22, p. 1-11.

Liu, J., Crowley, T.J., and Quinn, T.M., 2005, Breakdown of the Sr/Ca paleothermometer in a coral record from New Georgia, Western Pacific Warm Pool [abs.]: *Eos (Transactions, American Geophysical Union)*, v. 86, Fall Meet. Suppl., Abstract PP44A-07.

Marshall, J.F., and McCulloch, M.T., 2002, An assessment of the Sr/Ca ratio in shallow water hermatypic corals as a proxy for sea surface temperature: *Geochimica et Cosmochimica Acta*, v. 66, p. 3263-3280.

- Min, G.R., Edwards, R.L., Taylor, F.W., Récy, J., Gallup, C.D., and Beck, J.W., 1995, Annual cycles of U/Ca in coral skeletons and U/Ca thermometry: *Geochimica et Cosmochimica Acta*, v. 59, p. 2025-2042.
- Rayner, N.A., Parker, D.E., Horton, E.B., Folland, C.K., Alexander, L.V., Rowell, D.P., Kent, E.C., and Kaplan, A., 2003, Global analyses of sea surface temperature, sea ice, and night marine air temperature since the late nineteenth century: *Journal of Geophysical Research*, v. 108, 4407, doi: 10.1029/2002JD002670.
- Ren, L., Linsley, B.K., Wellington, G.M., Schrag, D.P., and Hoegh-Guldberg, O., 2002, Deconvolving the $\delta^{18}\text{O}$ seawater component from subseasonal coral $\delta^{18}\text{O}$ and Sr/Ca at Rarotonga in the southwestern subtropical Pacific for the period 1726 to 1997: *Geochimica et Cosmochimica Acta*, v. 67, p. 1609-1621.
- Schmidt, G.A., Bigg, G.R., and Rohling, E.J., 1999, Global Seawater Oxygen-18 Database, <http://data.giss.nasa.gov/o18data/>.
- Smith, T.M., and Reynolds, R.W., 2004, Improved extended reconstruction of SST (1854-1997): *Journal of Climate*, v. 17, p. 2466-2477.
- Suzuki, A., Hibino, K., Iwase, A., and Kawahata, H., 2005, Intercolony variability of skeletal oxygen and carbon isotope signatures of cultured *Porites* corals: Temperature-controlled experiments: *Geochimica et Cosmochimica Acta*, v. 69, p. 4453-4462.
- The Japanese Coral Reef Society and Ministry of the Environment, editors, 2004, *Coral Reefs of Japan*: Tokyo, Ministry of the Environment, 356 p.
- Woodhouse, C.A., Kunkel, K.E., Easterling, D.R., and Cook, E.R., 2005, The twentieth-century pluvial in the western United States: *Geophysical Research Letters*, v. 32, L07701, doi: 10.1029/2005GL022413.

Figure Legends

Figure DR1. X-radiographs of the *Porites* coral core. X-radiograph positive prints of 6-mm-thick slabs of core OGA-02-1. Alternating bands of high (dark colour) and low skeletal density (light colour) are visible. A high-density (summer)/low-density (winter) band pair represents one year. Corresponding years of coral growth are indicated. The sampling transect appears as a white line. Core length: 1.74 m, core diameter: 5.5 cm.

Figure DR2. Sea level pressure difference between the periods after and before the 1905-1910 freshening. Difference in average sea level pressure (SLP) (Basnett and Parker, 1997) between 1910-1942 minus 1873-1905 for winter (December, January, February) (**A**), summer (June, July, August) (**B**) and annual average conditions (**C**). Climatological surface winds, which are weakened by the anomalous atmospheric circulation resulting from the SLP anomaly pattern that is characterized by maximum gradients across southern Japan, are schematically represented as white arrows. Units: hPa. White dot: The Ogasawara Islands.

Figure DR3. Coral-based salinity of the western subtropical North Pacific and sea level pressure for different regions. Residual coral $\delta^{18}\text{O}$ records ($\Delta\delta^{18}\text{O}$) based on $\delta^{18}\text{O}$ and Sr/Ca, and $\delta^{18}\text{O}$ and U/Ca; coral-based sea surface salinity (SSS) anomaly calculated from regional $\delta^{18}\text{O}_{\text{seawater}}$ -salinity relationship (0.42‰/1 psu) (Schmidt et al., 1999); and regional SSS from SODA reanalysis (Carton and Giese, 2008) (142.0°-142.5° E, 27.0°-27.5° N), instrumental SSS axis is visually scaled (**A**). Sea level pressure (Basnett and Parker, 1997) over northeast Asia (110°-130° E, 45°-60° N) for winter (December, January, February) (**B**) and over the western subtropical North Pacific (145°-165° E,

20°-30° N) for summer (June, July, August) (C). Thin lines are annual records, bold lines are 3-year running averages. The grey bar indicates the time interval 1905-1910.

Figure DR4. Spectral properties of the coral-based salinity reconstruction from the western subtropical North Pacific. Results of multitaper method spectral analysis with red noise null hypothesis (Ghil et al., 2002) (number of tapers: 3; bandwidth parameter: 2) for coral $\Delta\delta^{18}\text{O}_{\text{Sr/Ca}}$ (A) and coral $\Delta\delta^{18}\text{O}_{\text{U/Ca}}$ (B) (1873-1994). The period (in years) for significant peaks (99%, 95% and 90% significance levels are shown) is indicated. Spectral analyses were performed for annual, detrended and normalized time series.

Figure DR5. Coral-based salinity of the western subtropical North Pacific and climate reconstructions from other locations. (A) Residual coral $\delta^{18}\text{O}$ records ($\Delta\delta^{18}\text{O}$) based on $\delta^{18}\text{O}$ and Sr/Ca, and $\delta^{18}\text{O}$ and U/Ca; coral-based sea surface salinity (SSS) anomaly calculated from regional $\delta^{18}\text{O}_{\text{seawater}}$ -salinity relationship (0.42‰/1 psu) (Schmidt et al., 1999); and regional SSS from SODA reanalysis (Carton and Giese, 2008) (142.0°-142.5° E, 27.0°-27.5° N), instrumental SSS axis is visually scaled. (B) Reconstruction of the summer Palmer Drought Severity Index (PDSI) for the western United States (Woodhouse et al., 2005). (C) Reconstruction of the Pacific Decadal Oscillation (PDO) index based on proxy data from the entire Pacific (Gedalof et al., 2002). Thin lines are annual records, bold lines are 3-year running averages. The grey bar indicates the time interval 1905-1910.

Figure DR6. Bimonthly resolved records of stable isotopes and elemental ratios from a western subtropical North Pacific coral. Bimonthly coral $\delta^{18}\text{O}$ (A), Sr/Ca (B), U/Ca (C)

and $\delta^{13}\text{C}$ (**D**) records. The yellow bar indicates the time interval 1995-2002 that was not used for climate reconstruction due to a breakdown of the coral Sr/Ca and U/Ca paleothermometers.

Figure DR7. Interannual records of elemental ratios, stable isotopes, paleosalinity and growth rate from a western subtropical North Pacific coral. (**A**) Coral Sr/Ca and U/Ca records, and local sea surface temperature (SST) at Chichijima (Tokyo Metropolitan Ogasawara Fisheries Center). (**B**) Regional SST estimates (Rayner et al., 2003; Smith and Reynolds, 2004) (ERSST2: 141°-143° E, 27°-29° N; HadISST1.1: 142°-143° E, 27°-28° N). (**C**) Coral $\delta^{18}\text{O}$ record. (**D**) Residual coral $\delta^{18}\text{O}$ records ($\Delta\delta^{18}\text{O}$) based on $\delta^{18}\text{O}$ and Sr/Ca, and $\delta^{18}\text{O}$ and U/Ca; coral-based sea surface salinity (SSS) anomaly calculated from regional $\delta^{18}\text{O}_{\text{seawater}}$ -salinity relationship (0.42‰/1 psu) (Schmidt et al., 1999); and regional SSS from SODA reanalysis (Carton and Giese, 2008) (142.0°-142.5° E, 27.0°-27.5° N). (**E**) Residual coral $\delta^{18}\text{O}$ records ($\Delta\delta^{18}\text{O}$) based on $\delta^{18}\text{O}$ and ERSST2, and $\delta^{18}\text{O}$ and HadISST1.1; and regional SSS (Carton and Giese, 2008). (**F**) Coral $\delta^{13}\text{C}$ and growth rate records. Instrumental SST and SSS axes are visually scaled. Thin lines are annual records, bold lines are 3-year running averages. The grey bar indicates the time interval 1905-1910. The yellow bar indicates the time interval 1995-2002 that was not used for climate reconstruction due to a breakdown of the coral Sr/Ca and U/Ca paleothermometers.

Figure DR8. Thin-section photomicrographs of the western subtropical North Pacific coral. Thin section of coral skeleton representing the year 1902 under transmitted light (**A**) and cross-polarized light (**B**). Thin section of coral skeleton representing the year

1913 under transmitted light (C) and cross-polarized light (D). No secondary aragonite cements are observed in the skeletal pore spaces, resulting in excellent preservation of primary porosity. Note the similarity in skeleton preservation prior and after the 1905-1910 freshening shift.

Figure DR9. Scanning electron microscope (SEM) images of the western subtropical North Pacific coral. SEM images of coral skeleton representing the year 1902 (A-D) and of coral skeleton representing the year 1913 (E-H). No secondary aragonite cements are observed in the skeletal pore spaces, resulting in excellent preservation of primary porosity. Skeletal walls and centres of calcification are easily identified. Primary aragonite fibres are clear and form a fan around a centre of calcification. Note the similarity in skeleton preservation prior and after the 1905-1910 freshening shift.

Figure DR10. Bimonthly resolved records of stable isotopes from a western subtropical North Pacific coral. Bimonthly coral $\delta^{18}\text{O}$ (A) and $\delta^{13}\text{C}$ (B) records of core OGA-02-1 (vertical growth) and core OGA-02-3 (horizontal growth) both drilled from the same *Porites* colony. Whereas the average coral $\delta^{18}\text{O}$ values are nearly identical the average coral $\delta^{13}\text{C}$ values show a clear offset. This indicates that effects of growth axis changes on coral $\delta^{18}\text{O}$ are negligible in this colony. The more negative coral $\delta^{13}\text{C}$ values of core OGA-02-3 can be explained by less photosynthetic activity of the coral's endosymbiotic algae due to reduced light availability at the side of the colony where this core was drilled, compared to core OGA-02-1 that was drilled at the top of the colony.

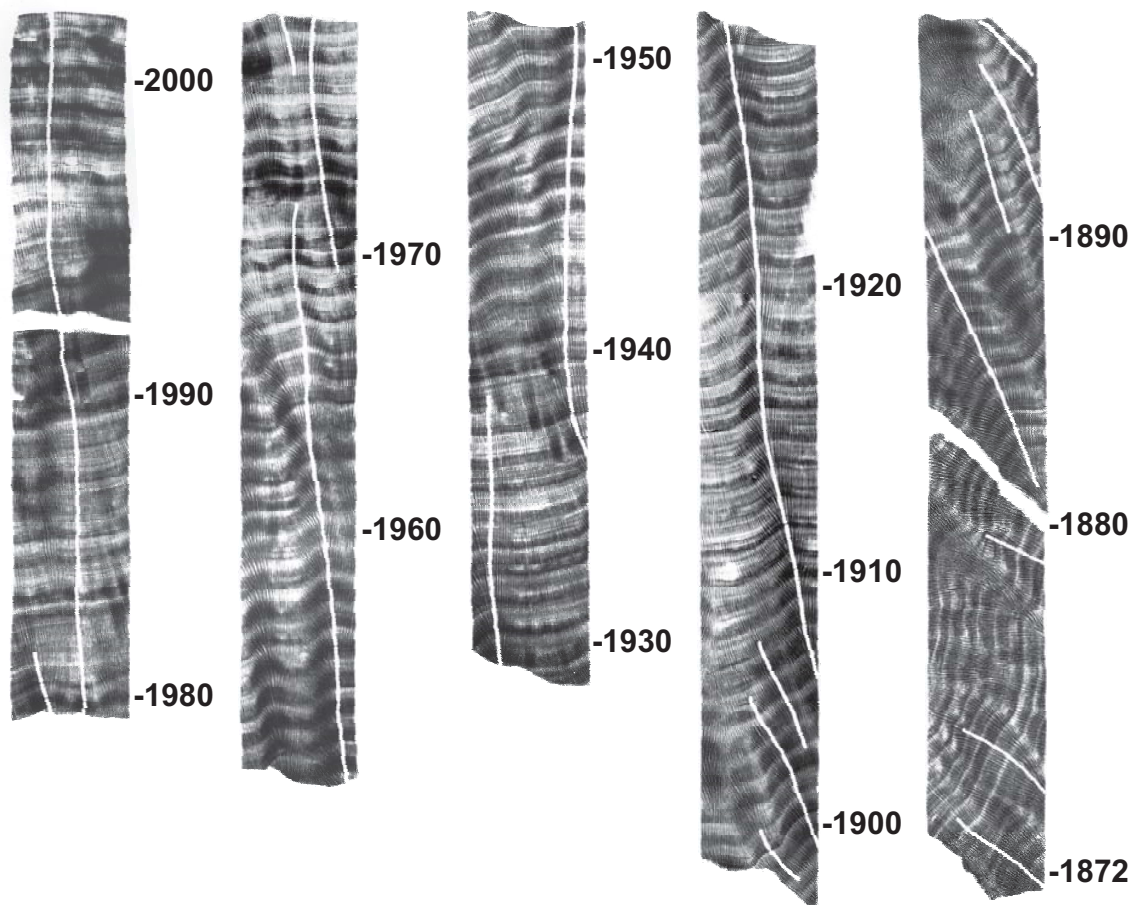


Figure DR1

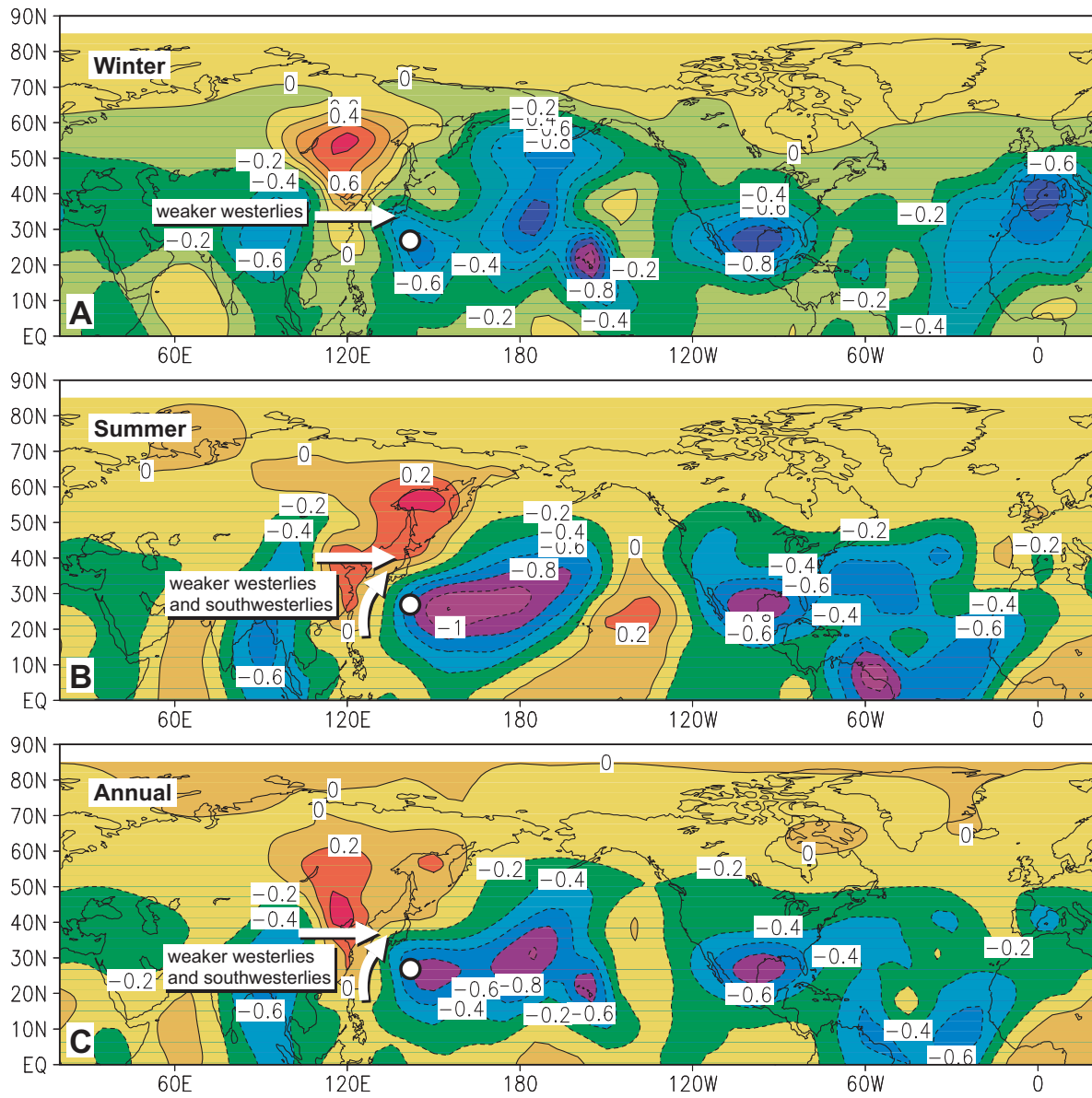


Figure DR2

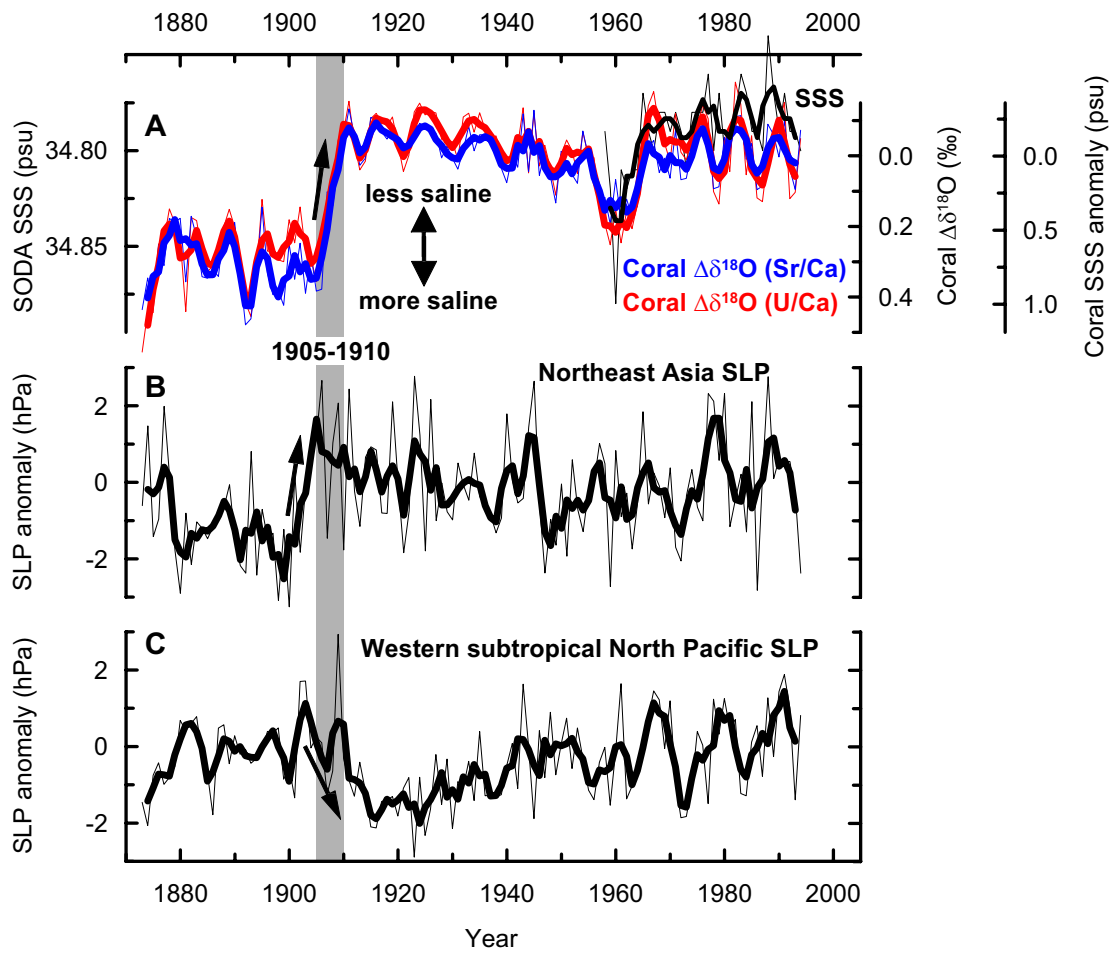


Figure DR3

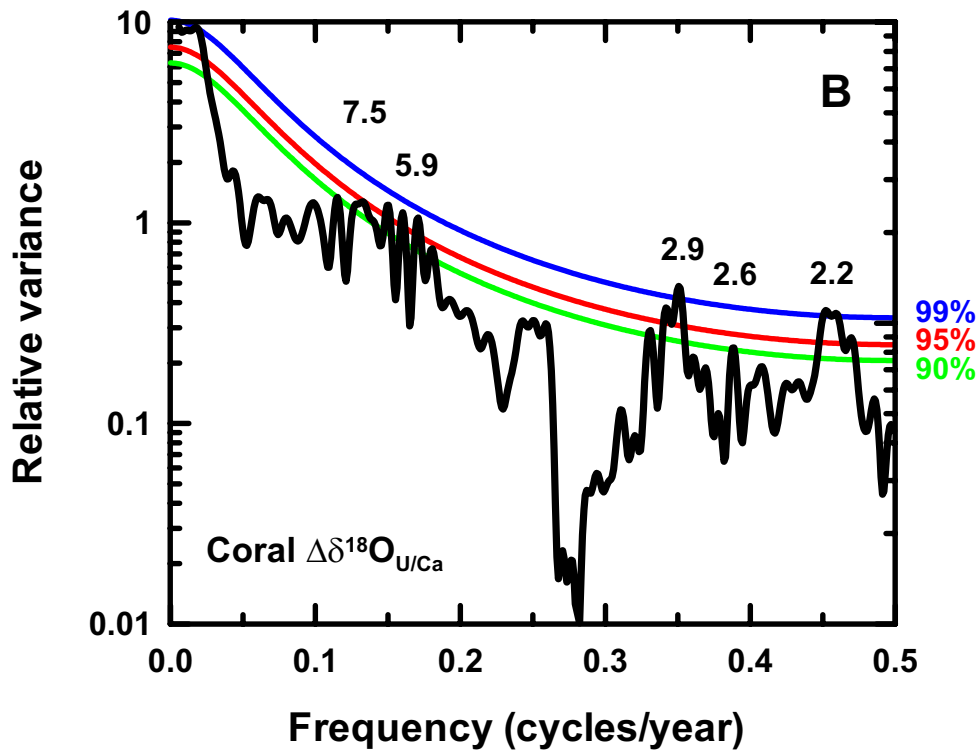
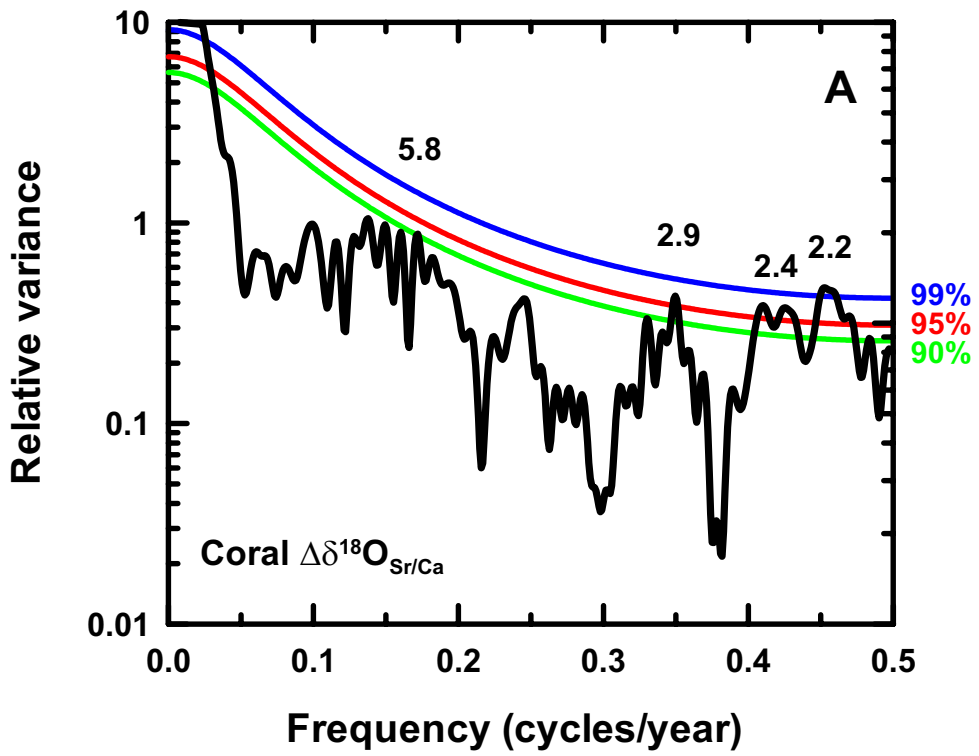


Figure DR4

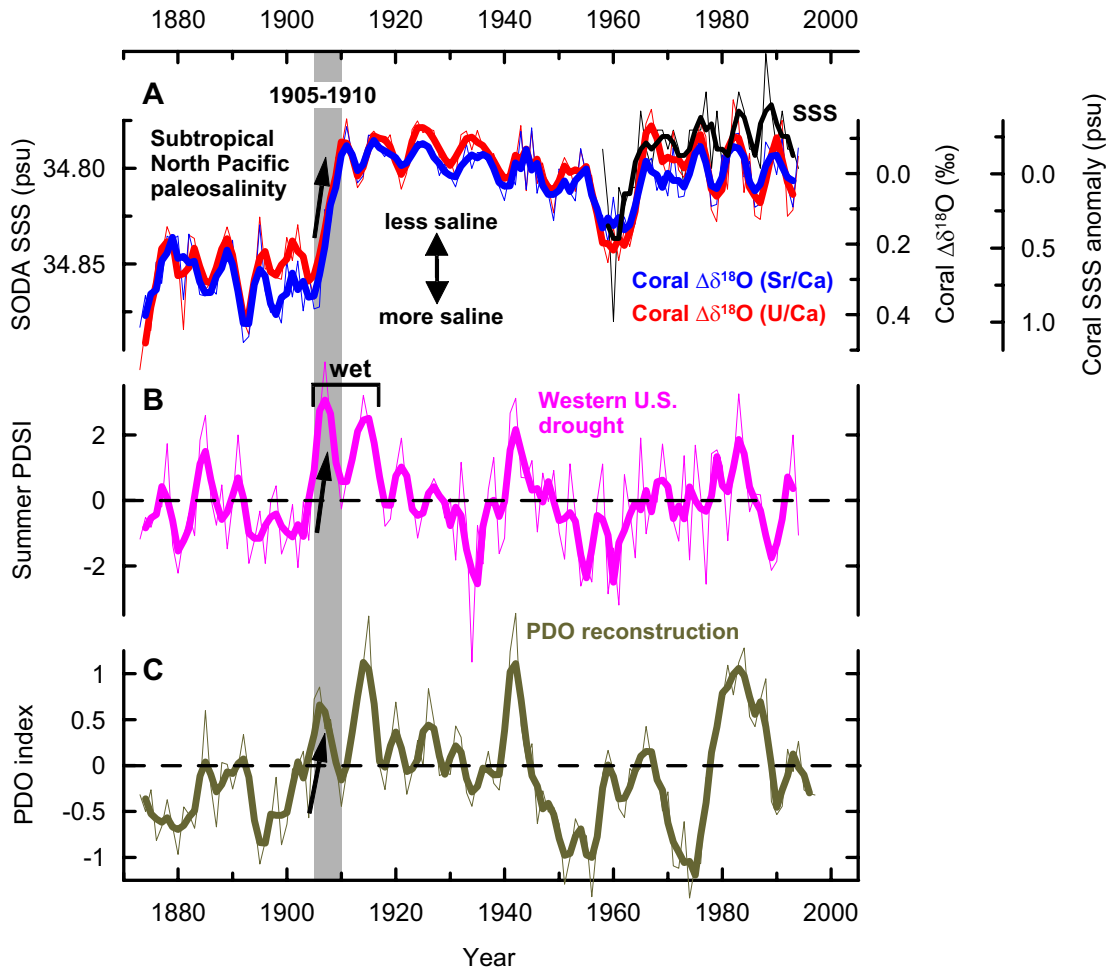


Figure DR5

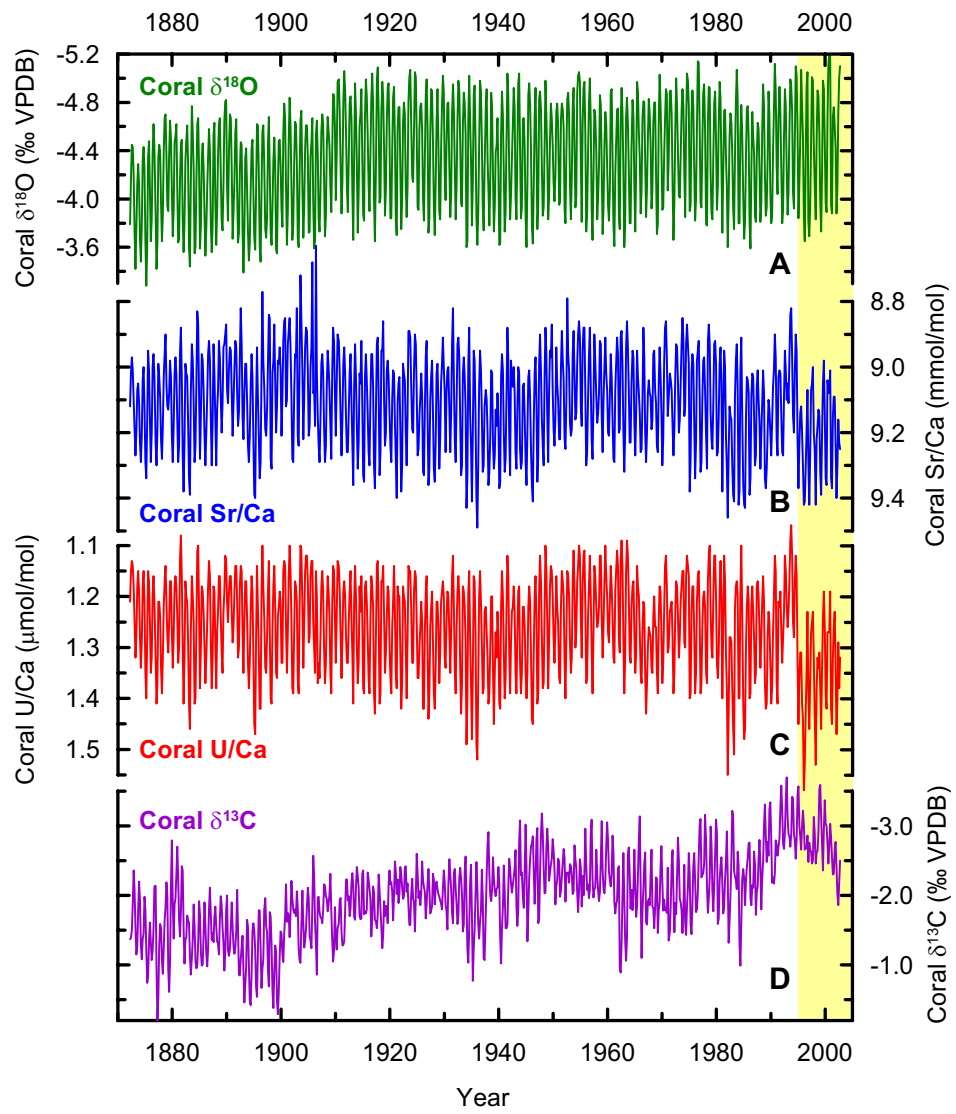


Figure DR6

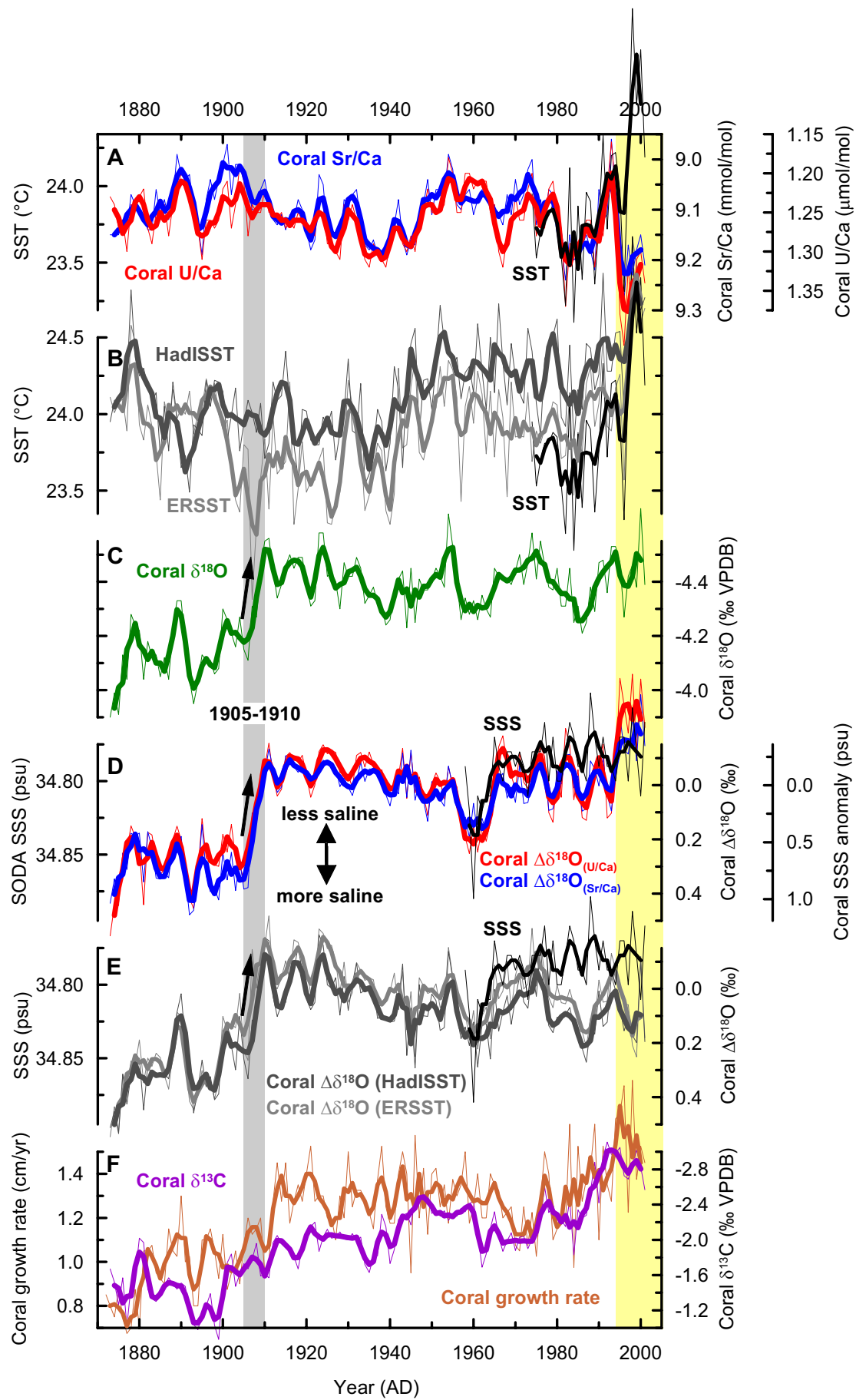


Figure DR7

1902

1913

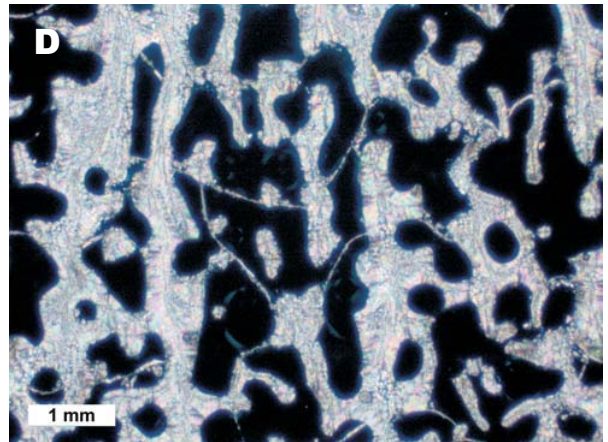
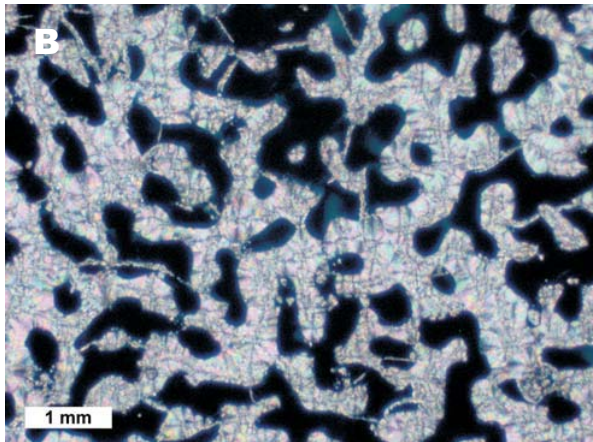
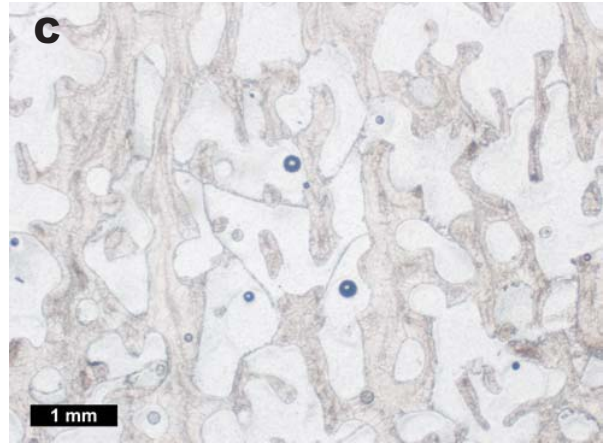
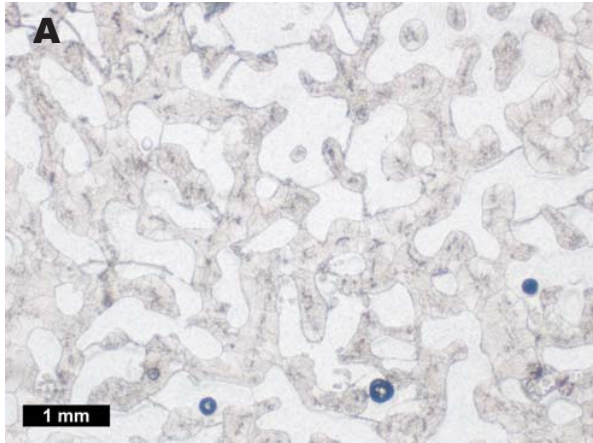


Figure DR8

1902

1913

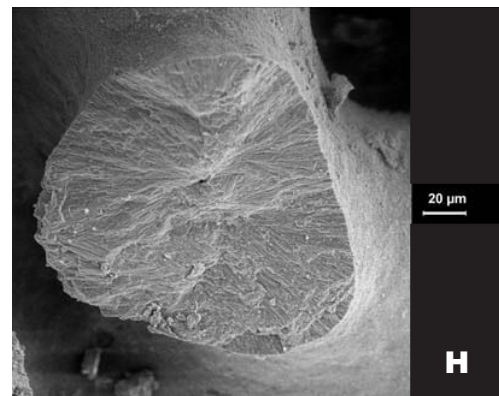
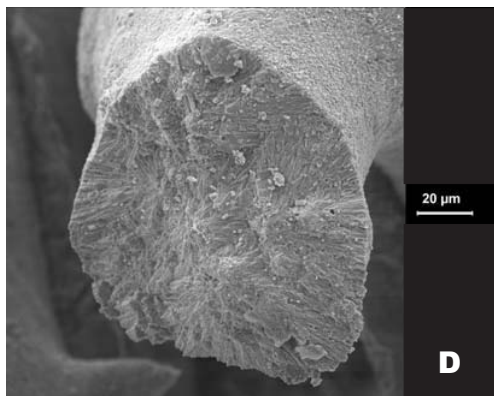
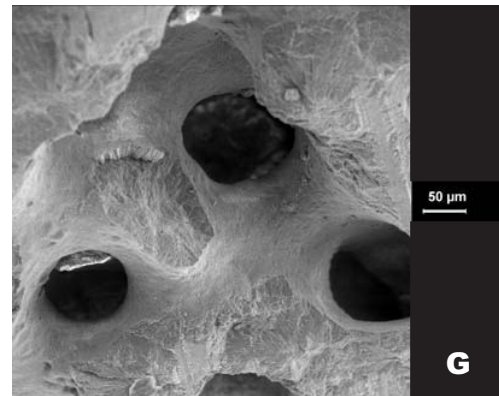
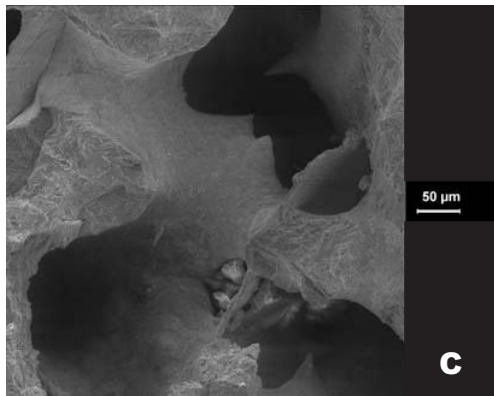
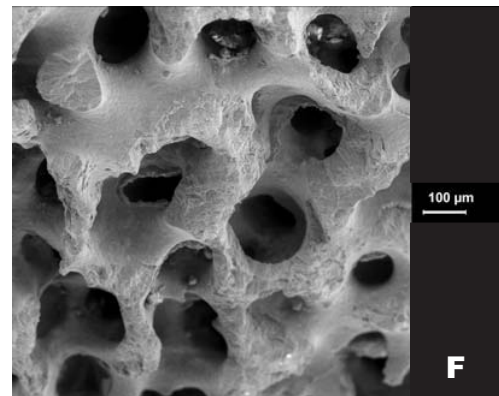
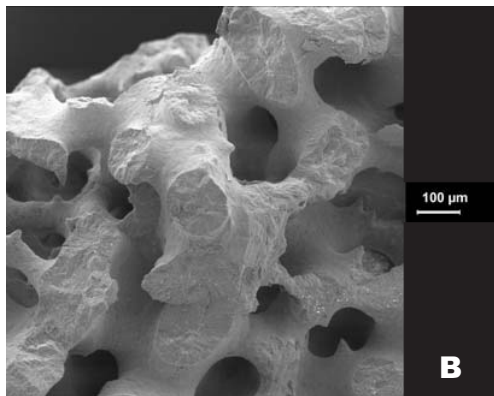
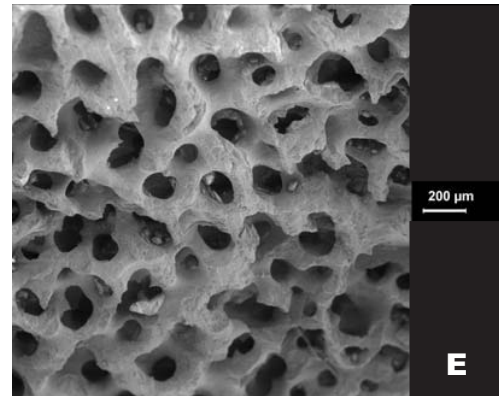
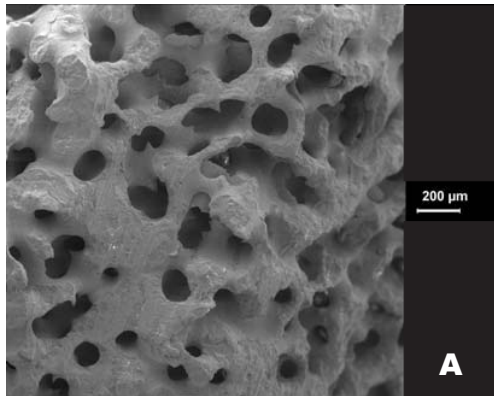


Figure DR9

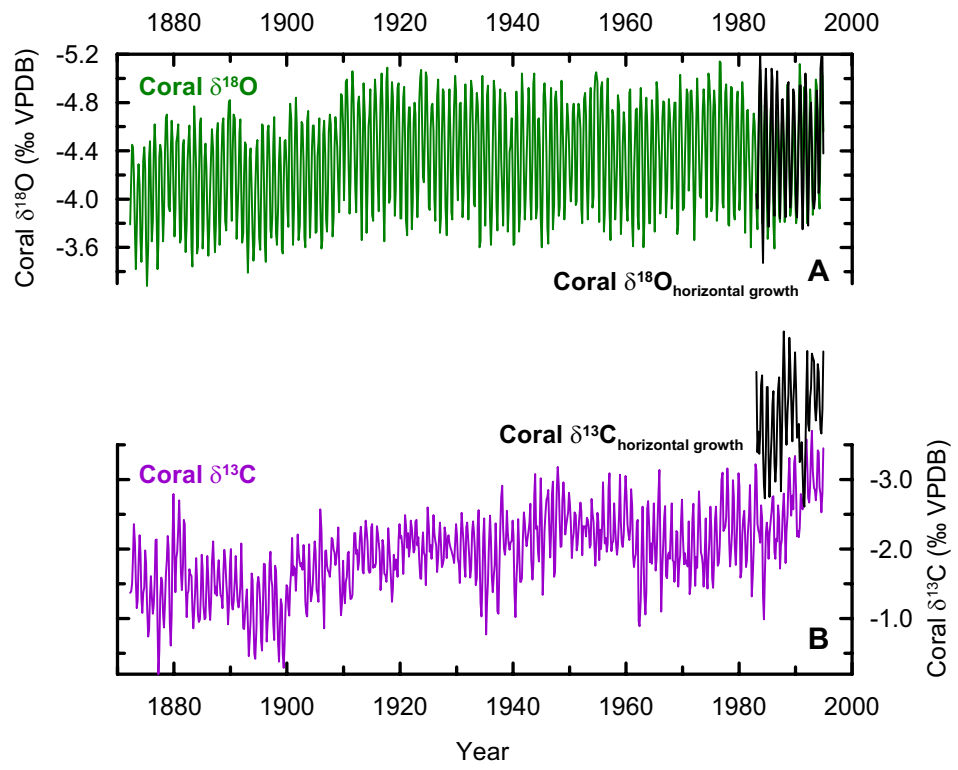


Figure DR10